BIOCHEMISTRY

Rapid Reports

Structural and Functional Studies Indicate That Shigella VirA Is Not a Protease and Does Not Directly Destabilize Microtubules[‡]

Katherine L. Germane,[§] Ryoma Ohi,[§] Marcia B. Goldberg,[||] and Benjamin W. Spiller*,[§]

Department of Pharmacology, Vanderbilt University Medical Center, 461 Preston Research Building, 2220 Pierce Avenue, Nashville, Tennessee 37232, Department of Microbiology and Immunology, Vanderbilt University Medical Center, 461 Preston Research Building, 2220 Pierce Avenue, Nashville, Tennessee 37232, Department of Cell and Developmental Biology, Vanderbilt University Medical Center, 3120B MRB III, 465 21st Avenue South, Nashville, Tennessee 37232, and Massachusetts General Hospital and Harvard Medical School, 65 Landsdowne Street, Room 423, Cambridge, Massachusetts 02139

ABSTRACT: VirA, an essential virulence factor in *Shigella* disease pathogenesis, is involved in the uptake, motility, and cell-to-cell spread of *Shigella* organisms within the human host. These functions have been attributed to a VirA protease activity and a mechanism of microtubule destruction via tubulin degradation [Yoshida, S., et al. (2006) *Science 314*, 985–989]. We report functional and crystallographic data indicating a novel VirA structure that lacks these activities but highlights the homology to the EspG virulence factor of pathogenic *Escherichia coli.*

Shigella sp. are the causative agents of the severe bacillary dysentery, shigellosis, which is responsible for ∼1.1 million deaths per year (*2*). An early step of infection is invasion of the intestinal lining by *Shigella* via entry into the basolateral side of intestinal epithelial cells. *Shigella* sp. use a type three secretion system (TTSS) to release virulence factors into the cytosol for cell invasion. Among other effects, the virulence factors cause major rearrangement of the host cell cytoskeleton, which induces membrane ruffling and phagocytosis of the bacterium. The virulence factor VirA is important for cell entry, actin-based motility within cells, and cell-to-cell spread (*3*). The VirA homologues EspG and EspG2 are weakly conserved (∼13–20% identical) in the closely related organisms *Escherichia coli* and *Citrobacter rodentium*. The low degree of conservation is functionally important, in that EspG, EspG2, and VirA can functionally substitute for each other (*4, 5*), despite the fact that *E. coli* and *C. rodentium* are noninvasive pathogens that induce rearrangements of the cellular cytoskeleton from outside the cell (*6–9*).

To investigate the biochemistry underlying VirA function, we have expressed and crystallized full-length and N-terminally truncated VirA from *Shigella flexneri*. All truncations up to residue 44 expressed well and were monomeric as judged by analytical gel filtration. Limited proteolysis and mass spectrometry reveal the first ∼44 amino acids to be disordered, consistent with the dramatic improvement in crystal quality realized by truncation of the first 44 amino acids. Crystals of full-length VirA diffracted to ∼4 Å and were severely twinned. The Δ44 construct crystallized and diffracted to 2.4 Å. The structure was determined by MIRAS using a mercury derivative and crystals of Se-methionine-substituted VirA. There are two molecules in the asymmetric unit, and the structure includes residues 53–326 and 340–399 of molecule A and residues 52–326 and 339–399 of molecule B. The N-terminus and residues 327–339 are not visible and presumed to be disordered. The two molecules are very similar to each other. The individual domains align with rms differences of 0.03 Å for the N-terminal domain,
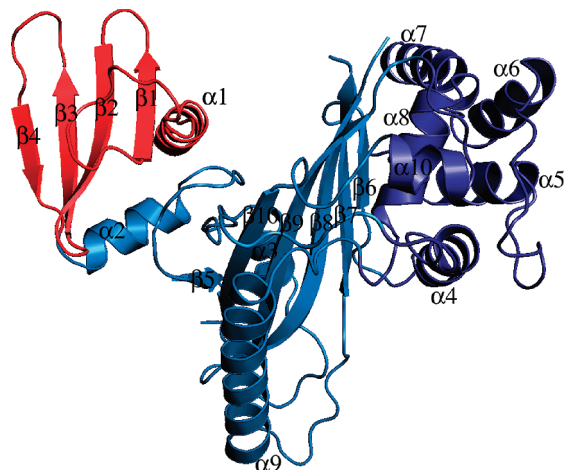
FIGURE 1: Ribbon diagram of VirA. The N-terminal domain is colored red and the C-terminal domain blue. The helical C-terminal subdomain is colored dark blue.

0.38 Å for the central sheet, and 0.54 Å for the C-terminal helical subdomain. Additionally, there is a 5° rotation between the N-terminal domain and the rest of the molecule, resulting in an overall rms difference of 1.95 Å for all main chain atoms. Data collection and refinement statistics are given in Table 1 of the Supporting Information.

The crystal structure reveals VirA to be a V-shaped molecule with a prominent cleft between the N- and C-terminal domains (Figure 1). Ten α-helices and 10 β-strands, in the form of two β-sheets, comprise VirA. The N-terminal domain is a flat four-stranded sheet, with helices at the N- and C-termini. This domain is connected to the rest of VirA by its C-terminal helix and a loop.

Consistent with a lack of mobility between these domains, the packing between the N-terminal domain and the rest of VirA appears to be quite tight, as judged by the low B-factors (relative to the rest of VirA) of the packing interface and the lack of solvent accessibility between the domains (Figure 1 of the Supporting Information). The first helix, α1, protrudes from the rest of VirA, making no contacts with the rest of the protein until residue 60, consistent with a lack of structure in the extreme N-terminus.

The central structure of VirA is a six-stranded sheet buttressed by eight helices and represents a large portion of the C-terminal domain. The sheet is curved, forming a convex surface between the N- and C-terminal domains. Helix α3 lies on the convex surface, partially filling the convex face. However, a prominent cleft still exists between the N-terminal domain and the rest of VirA with dimensions ~20 Å (depth) × 15 Å (width) × 20 Å (length). The C-terminal domain also contains a three-helix bundle formed by residues 208−267, which extends the face of the interdomain cleft formed by the N-terminal and central domains.

To assess VirA's structural homology to other proteins, we submitted the VirA coordinates to the DALI, VAST, and SSM webservers (10−13). The results indicate only very short regions of structural similarity (two secondary structural elements and a loop), indicating that VirA represents a novel fold, without substantial structural or sequence homology to any previously determined structure. The N-terminal domain, which on the basis of biochemical assays, has been reported to be a papain-like protease (1), lacks structural
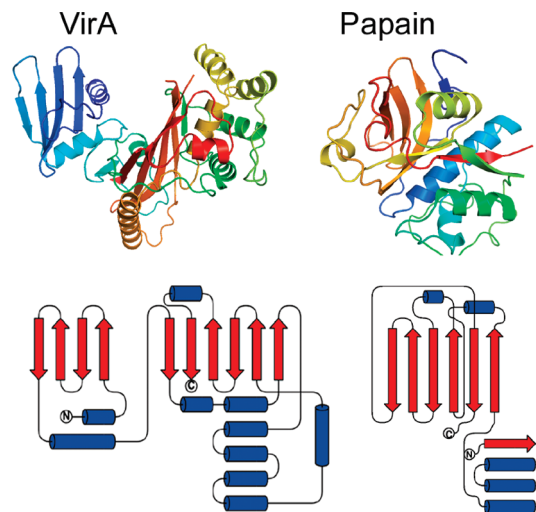

FIGURE 2: Comparison of VirA and papain structures. Ribbon diagrams of VirA (left) and papain (right) and topology diagrams of VirA (left) and papain (right). The VirA N-terminal domain and papain both contain four-stranded antiparallel sheets; however, the sheet in VirA is flat, and the sheet in papain is highly curved and is alternatively described as a part of a β-barrel or as a sheet (14, 15).
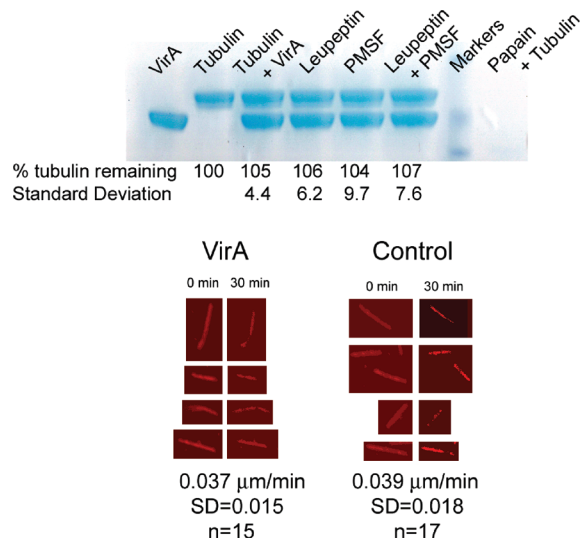

FIGURE 3: (a) Coomassie-stained SDS−PAGE showing VirA's inability to digest tubulin. VirA and tubulin were incubated at 37 °C for 2 h. Gels from four experiments were quantified by densitometry and averaged. In addition to the proteins, PMSF (10 mM) and/or leupeptin (0.1 mg/mL) was added. No digestion is discernible. The last lane shows complete digestion of tubulin by papain under similar conditions. (b) Representative examples of microtubules treated with either an ~5-fold molar excess of VirA or buffer. Samples were imaged every 30 s for 30 min. Significant photobleaching is evident, but the depolymerization rate in unaffected by VirA.

homology to papain (Figure 2). Further, the putative active site nucleophile (Cys34) is in an unstructured region of VirA and is not conserved in EspG2 (Figure 2 of the Supporting Information).

The lack of structural evidence to support the protease function of VirA led us to directly test VirA's ability to degrade tubulin. As shown in Figure 3a, purified VirA does not cleave tubulin. These experiments were performed in quadruplicate using roughly stoichiometric quantities of presumed catalyst and substrate. VirA is also unable to promote the disassembly of fluorescently labeled microtu-

bules assembled from the nonhydrolyzable GTP analogue GMPCPP (Figure 3b). Rhodamine microtubules were incubated with either buffer or a 5-fold molar excess of VirA and imaged every 30 s for 30 min. The average rate of depolymerization was 0.037 μ/min for VirA ($n = 15$, standard deviation of 0.015) and 0.039 μ/min for the control ($n = 17$, standard deviation of 0.018). These values are in agreement with the published spontaneous depolymerization rate of 0.03 μ/min for GMPCPP microtubules (*16*) and are inconsistent with a model in which VirA directly depolymerizes microtubules.

Using a gentamicin protection assay, which determines the fraction of *Shigella* to reach the host cytosol and hence be protected from the membrane impermeable antibiotic (*17*), we have confirmed the cell entry defect of VirA null *S. flexneri* to be decreased ∼5-fold compared to that of the wild-type strain (*3*) (Figure 3 of the Supporting Information). This highlights VirA's importance in *Shigella* virulence, although it also implies a different role for EspG, since cell invasion is not a prominent feature of *E. coli* pathogenesis (*8*). Since both entry of *Shigella* and tight adherence of pathogenic *E. coli* involve rearrangements of the cell cytoskeleton, the common functional feature of the two proteins may be in modulation of cytoskeletal dynamics.

VirA is a member of the EspG gene family, composed of EspG1 and EspG2 from *E. coli*, EspG from *C. rodentium*, and VirA from *Shigella* species. Conservation within each species is nearly perfect, while conservation between families is quite limited (Figure 2 of the Supporting Information). VirA is only ∼20% identical to EspG from *E. coli* or *C. rodentium*. The two EspG families within *E. coli* are ∼43% identical, although functionally redundant (*5, 18*), and the *C. rodentium* EspG is ∼75% identical to EspG1 from *E. coli*. The level of pairwise identity between VirA and EspG2 is only 13%. There are insertions of five, six, and seven amino acids in VirA relative to EspG. Two of these insertions occur within β-strands, removing five of 10 amino acids from $\beta7$ and four of 13 amino acids from $\beta8$. An unstructured loop connects $\beta7$ and $\beta8$ in VirA such that the central sheet of the C-terminal domain of EspG may well be intact, albeit with a shortened loop between $\beta7$ and $\beta8$. EspG also contains conserved glycines in putative helices $\alpha4$ and $\alpha6$. The VirA structure combined with sequence alignment indicates that some structural differences are possible between VirA and EspG. However, the lack of numerous insertions within secondary structural elements is consistent with similar folds. Further studies are necessary to reconcile the low level of sequence conservation among EspG family members with the observation that members can functionally substitute for each other (*4, 5*).

The VirA structure and accompanying functional studies indicate that VirA is not a protease. Further, using purified components, we are unable to detect microtubule severing or depolymerization and conclude that such activity in cells is not due to direct interaction between VirA and microtubules. We do not rule out a mechanism in which VirA modulates the activity of an unknown microtubule depolymerase.

SUPPORTING INFORMATION AVAILABLE

Detailed methods, figures depicting the *B*-factor distribution of VirA, and a sequence alignment of VirA, EspG, and EspG2. This material is available free of charge via the Internet at http://pubs.acs.org.

REFERENCES

1. Yoshida, S., Handa, Y., Suzuki, T., Ogawa, M., Suzuki, M., Tamai, A., Abe, A., Katayama, E., and Sasakawa, C. (2006) *Science 314*, 985–989.
2. Kotloff, K. L., Winickoff, J. P., Ivanoff, B., Clemens, J. D., Swerdlow, D. L., Sansonetti, P. J., Adak, G. K., and Levine, M. M. (1999) *Bull. W. H. O.,* 651–666.
3. Uchiya, K., Tobe, T., Komatsu, K., Suzuki, T., Watarai, M., Fukuda, I., Yoshikawa, M., and Sasakawa, C. (1995) *Mol. Microbiol. 17*, 241–250.
4. Elliott, S. J., Krejany, E. O., Mellies, J. L., Robins-Browne, R. M., Sasakawa, C., and Kaper, J. B. (2001) *Infect. Immun. 69*, 4027–4033.
5. Smollett, K., Shaw, R. K., Garmendia, J., Knutton, S., and Frankel, G. (2006) *Microbes Infect. 8*, 2220–2227.
6. Deng, W., Li, Y., Vallance, B. A., and Finlay, B. B. (2001) *Infect. Immun. 69*, 6323–6335.
7. Barthold, S. W., Coleman, G. L., Jacoby, R. O., Livestone, E. M., and Jonas, A. M. (1978) *Vet. Pathol. 15*, 223–236.
8. Knutton, S., McConnell, M. M., Rowe, B., and McNeish, A. S. (1989) *Infect. Immun. 57*, 3364–3371.
9. Knutton, S., Baldwin, T., Williams, P. H., and McNeish, A. S. (1989) *Infect. Immun. 57*, 1290–1298.
10. Krissinel, E., and Henrick, K. (2004) *Acta Crystallogr. D60*, 2256–2268.
11. Panchenko, A. R., and Bryant, S. H. (2002) *Protein Sci. 11*, 361–370.
12. Novotny, M., Madsen, D., and Kleywegt, G. J. (2004) *Proteins 54*, 260–270.
13. Holm, L., and Sander, C. (1996) *Science 273*, 595–603.
14. Richardson, J. S. (1981) *Adv. Protein Chem. 34*, 167–339.
15. Murzin, A. G., Brenner, S. E., Hubbard, T., and Chothia, C. (1995) *J. Mol. Biol. 247*, 536–540.
16. Varga, V., Helenius, J., Tanaka, K., Hyman, A. A., Tanaka, T. U., and Howard, J. (2006) *Nat. Cell Biol. 8*, 957–962.
17. Elsinghorst, E. A. (1994) *Methods Enzymol. 236*, 405–420.
18. Shaw, R. K., Smollett, K., Cleary, J., Garmendia, J., Straatman-Iwanowska, A., Frankel, G., and Knutton, S. (2005) *Infect. Immun. 73*, 4385–4390.

BI801533K